IMPACT RESISTANCE OF COMPOSITE STRUCTURES

S. Mohammadi [1]

[1] Asst. Prof., Dept. of Civil Engineering, Faculty of Engineering.,
University of Tehran, Tehran, Iran.
Email: smoham@shafagh.ut.ac.ir

ABSTRACT

A new approach based concepts of the Discrete Element Method, is presented for impact resistance analysis of composites. The method is capable of analysing the progressive fracturing and fragmentation behaviour as well as potential post cracking interactions caused by the newly created crack sides and segments. The imminence of a material crack is monitored by an anisotropic Hoffman model . To avoid the mesh dependency of the results, a bilinear local softening model is also adopted in this study to account for release of energy and redistribution of forces which caused the formation of a crack. A special re-meshing method has been developed to geometrically model an individual crack by splitting the element, separating the failed node, creating new nodes and dividing the neighbouring elements to preserve the compatibility conditions. Several numerical simulations have been performed to assess the performance of the proposed algorithm which covers a variety of benchmark finite element tests, standard experimental data and practical applications.

KEYWORDS: Impact, Cracking, Composites, Delamination, Discrete Element Method

INTRODUCTION

The phenomenon of failure by catastrophic crack propagation poses problems in all applications. Therefore, the development of reliable models for determining the failure behaviour of growing advanced matrials are vitally important.

Numerical simulation of arbitrary shaped components is traditionally performed by the finite element techniques, which is rooted in the concepts of continuum mechanics and is not suited to general fracture propagation and fragmentation problems. In contrast, the discrete element method (DEM) is specifically designed to solve problems that exhibit strong discontinuities in material and geometric behaviour.

The discrete element method idealizes the whole medium into an assemblage of individual bodies, which in addition to their own deformable response, interact with each other (through a contact type interaction) to capture the characteristics of the discontinuum and to perform the same response as the medium itself.

In this paper, some of the main aspects of crack initiation/propagation procedures by DEM in typical problems of impact on composites are discussed. Testing some of the benchmark and practical problems will help in verifying the performance of the proposed algorithm.

Nowadays composite materials are widely used in manufacturing aircrafts, helicopters, cars, satellite systems, etc. especially because of their lightness, high strength-to-weight ratio, good damping characteristics, and high fatigue strength. Therefore, having aircrafts larger than the Boeing 747 and faster than the Concorde are not only possible but also a reality.

Recent studies show that "delamination" is one of the most dominant causes of damage in composites subjected to impact loading. Delamination highly increases the buckling risk and the local transverse impacts by adjacent plies increase stress concentration in the cracks corners. Therefore, the important role of the phenomenon in reduction of load bearing capacity and performance of a structure necessitates an accurate analysis of initiation and propagation of interlaminar cracks and behaviour of the structure after cracking.

The aim of this study is to develop a reliable numerical method for 3D delamination modelling based on the principles of plasticity, contact mechanics and fracture mechanics. A contact based methodology is employed for modelling and controlling of plies bonding/debonding. The interlaminar behaviour in post delamination phase, such as slipping and crack faces interactions, is also considered by contact mechanics mechanisms. Employing an algorithm based on 3D contact mechanics in delamination analysis of composites is a novel technique and a more accurate and reliable analysis of this complex behaviour is expected to be obtained. In addition to 3D contact models, a 3D anisotropic bonding model with strain softening behaviour has also been developed and implemented to
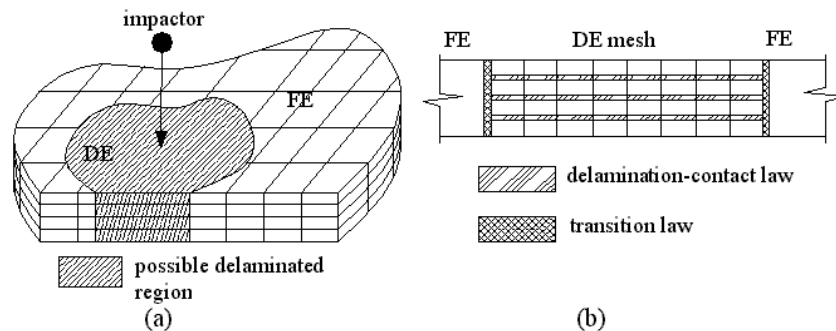

Figure 1: Composite specimen subjected to impact loading: (a) discrete/finite element mesh, (b) interfacial regions.

investigate interlaminar crack propagation.

1. ASPECT OF MODELLING OF COMPOSITE LAMINATES

In this study, modelling of a composite shell subjected to impact loading is performed by the use of finite/discrete element method. The possible delaminated region is modelled using discrete element mesh and the rest of the shell is modelled with coarser solid elements to reduce the analysis time (Fig. 1(a)). Each discrete element is discretized by a finite element mesh of equal or different sizes; finer mesh for the plies closer to the impact region and coarser mesh for the furthest ones. The interlaminar behaviour of plies such as debonding, impenetrability, friction and sliding determines connection conditions of the adjacent discrete elements (Fig. 1(b)). Discrete elements system and finite element mesh of the rest of the shell are connected together by transition interfaces which are defined as normal interfaces with very high bonding strengths which prevent debonding under all stress conditions. Non-linear material properties (using Hoffman anisotropic yield criterion) and geometric nonlinearities (large deformation) are also considered in the finite element formulation [3].

2. BOUNDARY VALUE PROBLEM AND FINITE ELEMENT FORMULATION

The dynamic boundary value formulation for a system consisting of the body of Ω with the boundary Γ can be expressed as

$$\mathscr{W}^{\text{inertia}} + \mathscr{W}^{\text{int.}} = \mathscr{W}^{\text{ext.}} + \mathscr{W}^{\text{con.}} \tag{1}$$

where the terms denote the virtual work of inertial forces, internal forces, external forces and contact forces respectively,

$$\mathscr{W}^{\text{inertia}} = \int_{\Omega} \delta \mathbf{u}^{\text{T}} \boldsymbol{\rho} \ddot{\mathbf{u}} \, d\Omega \tag{2}$$

$$\mathscr{W}^{\text{int.}} = \int_{\Omega} \delta \boldsymbol{\varepsilon}^{\text{T}} \boldsymbol{\sigma} \, d\Omega \tag{3}$$

$$\mathscr{W}^{\text{ext.}} = \int_{\Omega} \delta \mathbf{u}^{\text{T}} \mathbf{b} \, d\Omega + \int_{\Gamma_{\text{trac.}}} \delta \mathbf{u}^{\text{T}} \mathbf{t} \, d\Gamma + \int_{\Gamma_{\text{fix.}}} \delta \mathbf{u}^{\text{T}} \mathbf{r} \, d\Gamma \tag{4}$$

$$\mathscr{W}^{\text{con.}} = \int_{\Gamma_{\text{con.}}} \delta \mathbf{g}^{\text{T}} \boldsymbol{\sigma}^{\text{c}} \, d\Gamma \tag{5}$$

in which, $\Gamma_{\text{trac.}}$, $\Gamma_{\text{con.}}$ and $\Gamma_{\text{fix.}}$ are the region of traction forces, contact and fixed regions, respectively. $\boldsymbol{\rho}$ is the matrix of mass density, $\mathbf{b}$, $\mathbf{t}$ and $\mathbf{r}$ are the vectors of body forces, traction forces and reactions, respectively. $\boldsymbol{\sigma}$ and $\boldsymbol{\varepsilon}$ are the Cauchy stress and the strain tensors, $\mathbf{u}$ is the displacement vector, $\boldsymbol{\sigma}^{\text{c}}$ is the contact (interfacial) stress vector and finally, $\mathbf{g}$ denotes the contact gap vector.

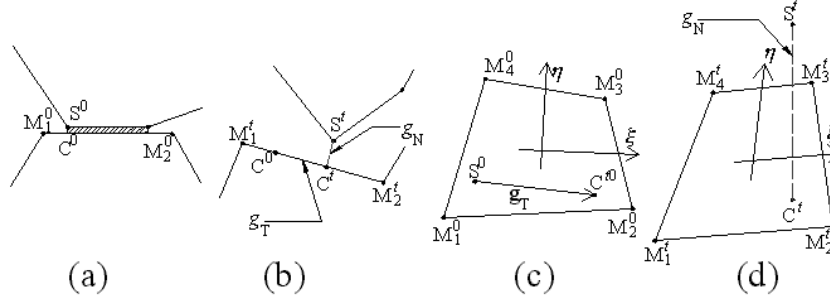Eqn. (1) can be rewritten in matrix form as

Figure 2: Normal and tangential gaps in 2D and 3D problems: (a) initial configuration (bounded plies) in 2D, (b) current configuration in 2D, (c) initial configuration (bounded plies), (d) current configuration in 3D.

$$\mathbf{M}\ddot{\mathbf{u}} + \mathbf{f}^{\text{int.}} = \mathbf{f}^{\text{ext.}} + \mathbf{f}^{\text{con.}} \tag{6}$$

where $\mathbf{M}$ denotes the mass matrix and $\mathbf{f}^{\text{int.}}$, $\mathbf{f}^{\text{ext.}}$, $\mathbf{f}^{\text{con.}}$ denote the internal, external and contact force vectors, respectively.

The explicit central difference method is employed due to the large amount of data and to prevent time-consuming iterations [4].

3. CONSTITUTIVE INTERFACIAL RELATIONSHIP

A bilinear strain-softening model [1, 2] together with The penalty method to impose impenetrability and frictional contact are employed in bonding interfaces. A contact gap vector can be described as

$$\mathbf{g} = \left[g_N, \mathbf{g}_T \right]^{\mathrm{T}} \tag{7}$$

where g_N is the normal distance between contactor node S and contact segment M_1M_2 in 2D or $M_1M_2M_3M_4$ in 3D. $\mathbf{g}_T$ is a tangential vector whose size is equal to the distance between the projection of the contact node in the current configuration and the initial configuration (Fig. 2). The components of the gap vector determine the state of two adjacent plies as shown in Table 1.

Table 1: PLIES STATES IN RELATION TO GAP CONDITIONS

Fracture Mode	Gap Condition	Plies State
Pure Mode I	$g_N < 0$	Penetration
	$0 < g_N < \bar{g}_{Nu}$	Opening without debonding
	$g_N > \bar{g}_{Nu}$	Opening of debonded plies
Pure Mode II	$g_T = \left\| \mathbf{g}_T \right\| < \bar{g}_{Tu}$	Shearing without cracking
	$g_T = \left\| \mathbf{g}_T \right\| > \bar{g}_{Tu}$	Friction and sliding of two debonded plies

Thus, combining the bilinear strain-softening model with The penalty method leads to constitutive interfacial relationship in pure modes I and II (Fig. 3), where g_T is the magnitude of vector $\mathbf{g}_T$, $\bar{\sigma}_t$ and $\bar{\sigma}_s$ are the threshold tensile and shear strength of the binder between plies while $\bar{g}_t$ and $\bar{g}_s$ are the related displacements. $\bar{g}_{Nu}$ and $\bar{g}_{Tu}$ are the maximum normal and tangential displacements, which the binder can bear without debonding. Fracture energy release rate for modes I and II are defined as
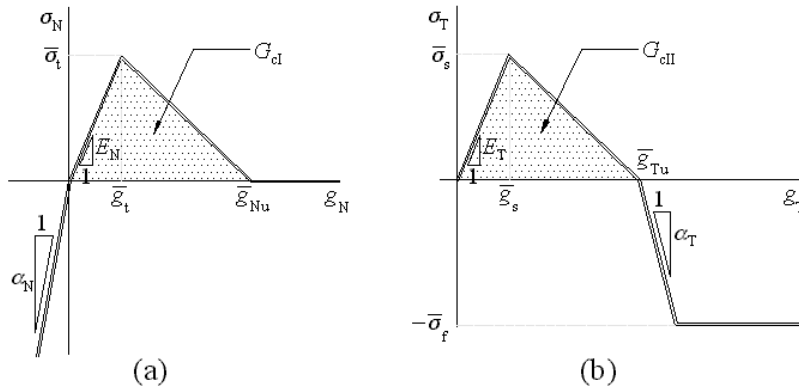

Figure 3: Normal and tangential contact stress—gap vector magnitude diagram.

the area under the normal and tangential stress-displacement curves respectively, that is

$$G_{cI} = \tfrac{1}{2}\bar{\sigma}_t\, \bar{g}_{Nu} \quad , \quad G_{cII} = \tfrac{1}{2}\bar{\sigma}_s\, \bar{g}_{Tu} \tag{8), (9}$$

So, $\bar{g}_{Nu}$ and $\bar{g}_{Tu}$ are known since G_{cI} and G_{cII} are assumed to be constant material properties and $\bar{\sigma}_t$ and $\bar{\sigma}_s$ can be obtained by experiments. α_N and α_T are the Penalty parameters and $\bar{\sigma}_f$ is the maximum friction stress between plies,

$$\bar{\sigma}_f = \mu \left\langle -\sigma_N \right\rangle \tag{10}$$

where μ is the Coulomb coefficient of dry friction and $\left\langle \bullet \right\rangle$ denotes the Macaulay function, that is

$$\langle x-a\rangle = \begin{cases} x-a & ; \; x\geq a \\ 0 & ; \; x<a \end{cases} \tag{11}$$

Fig. 3 shows the stress-displacement relationship in pure modes I and II. In practice however, initiation of delamination in any mode will affect on the other modes of fracture. Here, a coupled delamination damage model introduced by [2] has been employed in this study to include these effects. The model is based on the extent of damage, defined by:

$$\kappa = \sqrt{\left\langle \frac{g_N}{\overline{g}_t}\right\rangle^2 + \left(\frac{g_T}{\overline{g}_s}\right)^2} - 1 \tag{12}$$
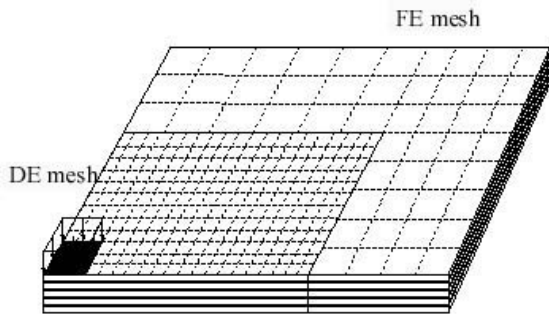
in which the use of the Macaulay function for the normal displacement is due to the fact that only tensile displacement (opening) affects on delamination. According to this model, delamination will initiate as soon as κ exceeds zero. Combination of this model and the Penalty method leads to the constitutive relationship between interfacial stresses and their related displacements, that is

$$\boldsymbol{\sigma}^c = \begin{bmatrix} \sigma_N & \sigma_T \end{bmatrix}^T = \mathbf{D}^c\,\mathbf{g} \quad, \quad \mathbf{D}^c = \text{Diag}\left[D_N^c(\mathbf{g}), D_T^c(\mathbf{g}), D_T^c(\mathbf{g})\right] \tag{13), (14}$$

Defining three parameters $S_N(\kappa)$, $S_T(\kappa)$ and g_{Tu}^* as

$$S_N(\kappa) = \frac{\kappa}{1+\kappa}\cdot\frac{\overline{g}_{Nu}}{\overline{g}_{Nu}-\overline{g}_t} \quad, \quad S_T(\kappa) = \frac{\kappa}{1+\kappa}\cdot\frac{\overline{g}_{Tu}}{\overline{g}_{Tu}-\overline{g}_s} \tag{15), (16}$$

$$g_{Tu}^* = \overline{g}_s\sqrt{\left\langle\left(\frac{\overline{g}_{Tu}}{\overline{g}_s}\right)^2 - \left\langle\frac{g_N}{\overline{g}_t}\right\rangle^2\right\rangle} \tag{17}$$

Model size $= 0.0762 \times 0.0508 \times 0.00444\,\text{m}$
Ply region $= \begin{bmatrix} 90_n, 0_n, 90_n, 0_n, 90_n \end{bmatrix}$
DE region $= 0.050 \times 0.035\,\text{m}$

$E_{xx} = 152.4\text{E3}\,\text{MPa}$	$E_{yy} = 10.7\text{E3}\,\text{MPa}$
$v = 0.35$	$\rho = 0.35\,\text{kg}/\text{m}^3$
$X_t = 2772\,\text{MPa}$	$X_c = 3100\,\text{MPa}$
$Y_t = 79.3\,\text{MPa}$	$Y_c = 231.0\,\text{MPa}$
$S = 132.8\,\text{MPa}$	

Figure 4: FE/DE mesh of one quarter of the composite specimen

results in

$$D_N^c(\mathbf{g}) = \begin{cases} \alpha_N & ; \quad g_N \leq 0 \\ E_N & ; \quad g_N > 0,\; \kappa \leq 0 \\ (1-S_N(\kappa))E_N & ; \quad g_N > 0,\; S_N(\kappa) < 1 \\ 0 & ; \quad g_N > 0,\; S_N(\kappa) \geq 1 \end{cases} \tag{18}$$

$$D_T^c(\mathbf{g}) = \begin{cases} E_T & ; \quad \kappa \leq 0 \\ \left(1 - S_T(\kappa)\right)E_T & ; \quad \kappa > 0, \, S_T(\kappa) < 1 \\ -\left(\dfrac{g_{Tu}^*}{g_T} - 1\right)\alpha_T & ; \quad S_T(\kappa) \geq 1, \, g_T < g_{Tu}^* + \dfrac{\overline{\sigma}_f}{\alpha_T} \\ \dfrac{\overline{\sigma}_f}{g_T} & ; \quad S_T(\kappa) \geq 1, \, g_T \geq g_{Tu}^* + \dfrac{\overline{\sigma}_f}{\alpha_T} \end{cases} \qquad (19)$$

4. NUMERICAL STUDIES

A composite plate specimen subjected to a triangular load applied from 0 to 5 μsec with a peak force of 5kN is investigated. This modelling is a numerical simulation of the experiments undertaken by [5]. Because of symmetry, only one quarter of the plate is modelled (Fig. 4). Also, only the central region of this model is meshed by discrete elements. To ensure the mesh independency of the results, the analysis is performed with both a coarse and a finer mesh. The deformed shape of the plate at $t = 0.00018$ sec is illustrated in Fig. 5(a). Fig. 5(b) depicts the comparison of the displacement history of the centre of the plate (both top and bottom points across the thickness) for both coarse and fine mesh. Also, Fig. 6 illustrates the delamination patterns of the top and bottom plies interfaces of the fine mesh at $t = 0.00012$ sec and $t = 0.00018$ sec.

It should be noted that these results were achieved without considering a material fracture analysis and only delamination was activated. In practice, however, the illustrated large deformation will certainly involve extensive material fracture and failure.

5. CONCLUSIONS

A contact based method has been successfully developed for 3D delamination modelling of composites. The initiation and propagation of delamination has been considered by using a bilinear strain-softening model, which has been found to be properly accurate. The Penalty method has been employed to impose impenetrability and post-debonding behaviours of plies. A numerical example has been successfully analysed with this approach. This method could easily be combined with an in-plane fracturing algorithm to perform a full fracturing analysis of composites subjected to impact loading.
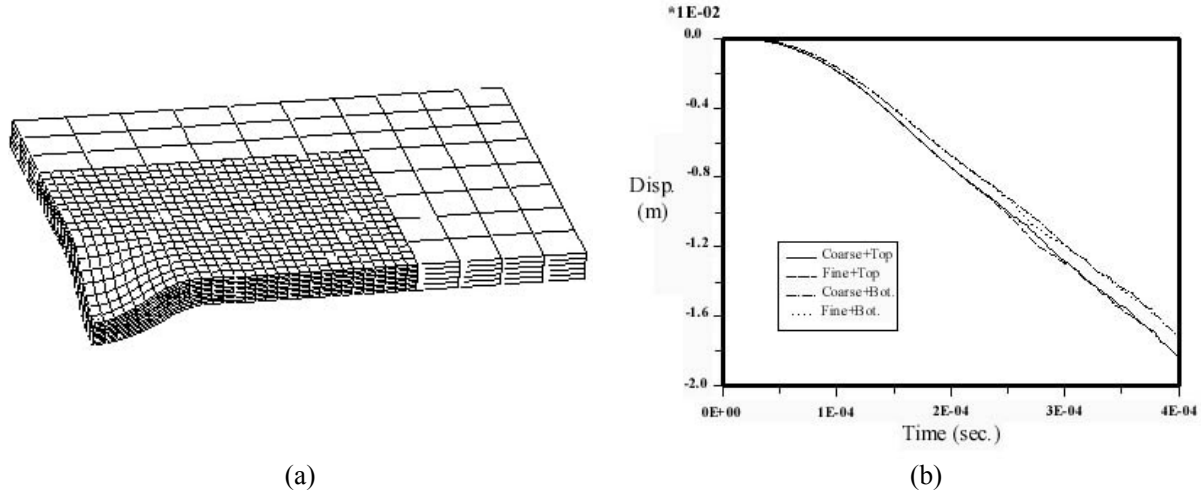

(a)   (b)

Figure 5: (a) Deformed shape of the plate at $t = 0.00018$ sec. (b) Displacement history of the central point.
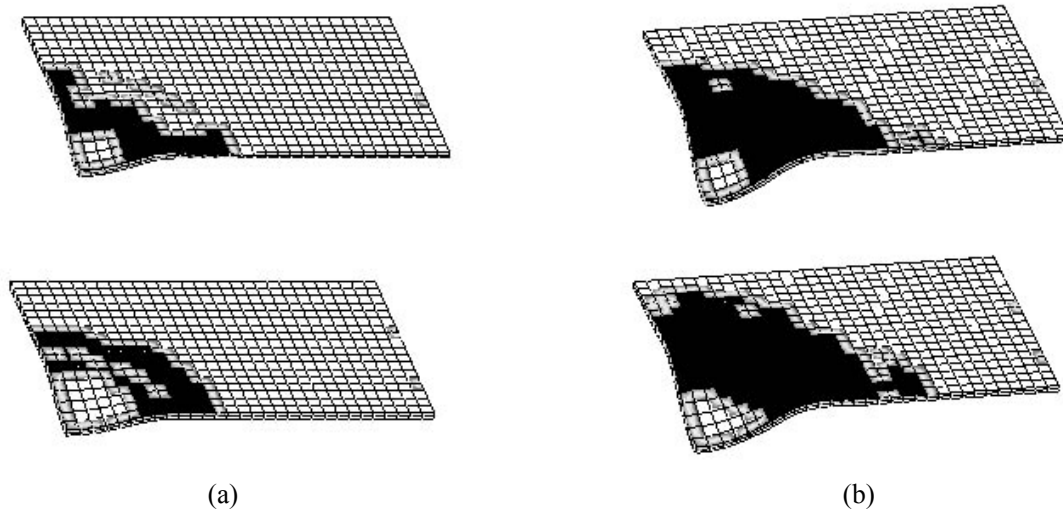
<div align="center">(a)   (b)</div>

Figure 6: Delamination patterns at the top and bottom plies interfaces of the finer mesh: at (a) $t = 0.00012$ and (b) $t = 0.00018 \, \text{sec}$.

REFERENCES

[1] Mi Y. and Crisfield M.A. (1996); "*Analytical Derivation of Load/Displacement Relationship for the DCB and MMB and Proof of the FEA Formulation*", IC-AERO Report 97-02, Dept. Aeronautics, Imperial College, London, UK.

[2] Mi Y., Crisfield M.A., Davies G.A.O. and Hellweg H.-B. (1998); "Progressive delamination using interface elements", *J. Composite Materials*, **32:14**, 1246-1272.

[3] Mohammadi S. (1998); "*Combined Finite/Discrete Element Analysis of Impact Loading of Composite Shells*", Ph.D. thesis, Dept. Civil Engineering, University of Wales Swansea, UK.

[4] Mohammadi S., Owen D.R.J. and Perić D. (1998); "A combined finite/discrete element algorithm for delamination analysis of composites", *Finite Elements in Analysis and Design*, **28**, 321-336.

[5] Worswick M.J., Strazincky P.V. and Majeed O. (1995); "Dynamic fracture of fibre reinforced composite coupons", in: Sun C.T., Sankar B.V. and Rajapakse Y.D.S. (editors), *Dynamic Response and Behaviour of Composites*, ASME AD: **46**, 29-41.